Tr. J. of Engineering and Environmental Science
22 (1998) , 185 – 195.

Heat Transfer and Flow Structure in a Rectangular Channel With Wing-Type Vortex Generator

İsak KOTCİOĞLU
Mechanical Engineering Department,
Atatürk University, Erzurum-TURKEY,
Teoman AYHAN, Hayati OLGUN, Betül AYHAN
Mechanical Engineering Department
Karadeniz Technical University, Trabzon-TURKEY,

Received 24.06.96

Abstract

A detailed evaluation of performance parameters in the turbulent regime with regard to the enhancement of heat transfer using winglet-type vortex generators has been accomplished in this study. The heat transfer characteristics and flow structure in turbulent flow throught a rectangular channel containing built-in wing type vortex generator, have been investigated experimentally in the range of Reynolds number between 3,000 and 30,000. The geometrical configuration of interest is reminiscent of single element of a plate-fin cross-flow heat exchanger. The installation of wings is organized, in such a way that periodically interrupted enlarged and contracted channel flow domains can be established. Thus, each inglet pair acts as periodically interrupted divergent and convergent short channels in a rectangular channel. Wings were aligned at various angles of β=7-20° positively and negatively with the direction of main air flow direction. Each winglet pair induce longitudinal vorticity behind it, and strong mixing effects occur in a buffer region between divergent and convergent channel arrangements. The vortices in these flow domains cause enhanced heat transfer. It is observed that, the enhancement of heat transfer caused the increment of the friction coefficient.

Key Words: Heat Transfer Enhancement, Wing Type Vortex Generator, Periodically Interrpted Winglets, Divergent and Convergent Short Channels, Turbulent Flow

İçerisinde Kanatçık Üreteçleri Bulunduran Dikdörtgen Kesitli Kanallarda Isı Transferi ve Akışın İncelenmesi

Özet

İçerisinde kanatçık tipi girdap üreteçleri bulunduran dikdörtgen kesitli kanallardaki ısı transferi, farklı Reynolds sayılarında (3000-30000) ve türbülanslı akış koşullarında deneysel olarak incelenmiştir. Bu çalışmada kullanılan girdap üreteçleri, levha-kanat tipli ve çapraz akışlı ısı değiştirgeçlerinde kullanılmaktadır. Kanatçıklar, periyodik olarak daralan ve genişleyen yapıda kanal içerisine yerleştirilmiştir. Böylelikle her bir kanatçık grubu, bir daralan ve bir genişleyen kısa kanallar oluşturmuştur. Kanatçıkların açısı, akış doğrultusu ile pozitif ve negatif olarak 7-20° arasında açı yapacak şekilde değiştirilebilmektedir. Kanatçık açılarının değişiminin ısı transferine etkileri deneysel olarak incelenmiş olup, her bir kanatçık çiftinin arkasındaki geçiş bölgelerinde kuvvetli bir akış karışımı gözlenmiştir. Bu akış karışımının, ısı transferinin iyileşmesine neden olduğu tespit edilmiştir. Isı transferindeki bu iyileşmeye karşılık sürtünme katsayısının arttığı görülmüştür.

Anahtar Sözcükler: Isı Transferini yileştirme, Kanatcık Tipli Vorteks Üreticisi, Periyodik Olarak Aralıklı Yerleştirilmiş Kanatlar, Daralan ve Genişleyen Kısa Kanallar, Türbülanslı Akış

Introduction

The subject of heat transfer is of serious interest in heat exchanger applications. The process industries call for more and more compact designs of heat exchangers. Flow interruption created in flow at periodic intervals is a popular means for heat transfer enhancement in compact heat exchangers. There have been a number of survey articles and handbook sections prepared that deal with the augmentation of heat transfer for different applications (Bergles 1978, 1983, 1985). Special turbulence promoter devices bring about the transport enhancement by establishing a higher heat transfer coefficient. Wing-type vortex generators can be mounted in between bottom and top walls of channel in order to generate vortices which disrupt the growth of the boundary layer and thereby enhance the heat transfer between the flowing fluid and channel walls. One relevant application using such flow configurations is the heat transfer between the flowing fluid and plates in the case of plate-fin heat exchangers, is shown in Fig. 1. Experimental investigations due to Russels et al. (1982) and Deb et al. (1995) can be referred to in connection with augmentation of heat transfer by means of wing-type vortices. For converging - diverging channels, Mendes and Sparrow (1984) performed and experimental study to determine the entry region and fully developed heat-transfer coefficient, pressure distribution and friction factor at various taper angles of the converging and diverging tubes. Garg and Maji (1988) report the results of numerical analysis for diverging-converging channels. These results demonstrate that the converging - diverging channel configuration is an effective technique for enhancing heat transfer. However, such a technique is accompanied by undesired increase in pressure drop.

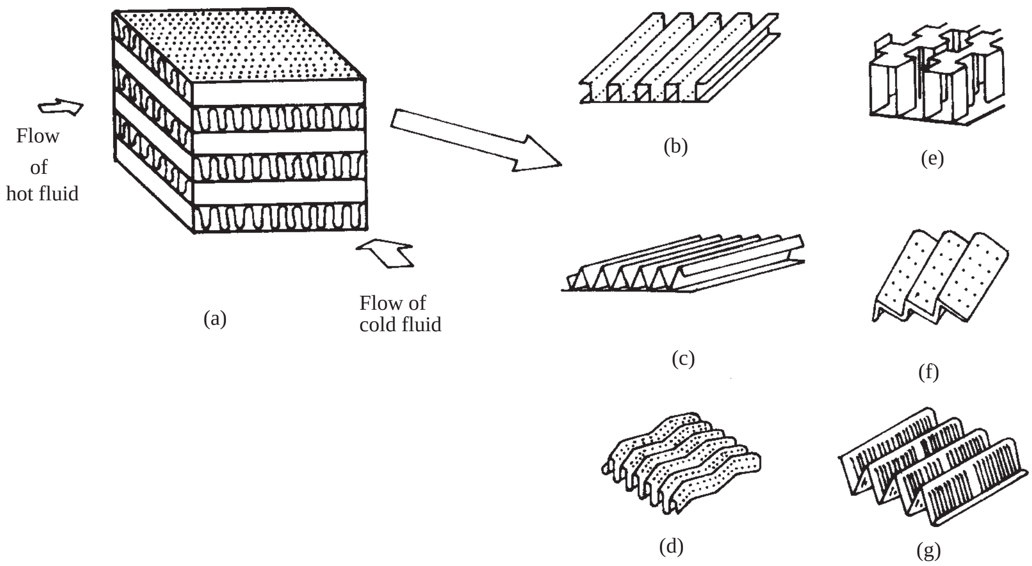

Figure 1. (a) Plate-fin heat exchanger and its surface geometries, (b) plain rectangular fins, (c) plain triangular fins, (d) wavy fins, (e) offset strip fins, (f) perforated fins and (9) louvered fins.

Fuji et al. (1988) proposed new enhanced surfaces for forced-convection heat transfer at low Reynolds number. The surface has many perforations and is bent to form a trapezoidal shape. Therefore, channels constructed with these surfaces have enlargement and contraction parts alternatively along the flow passages. They confirmed that substantial heat transfer enhancement is achieved by suction and injection flows throgh the perforations.

In the present paper, an experimental investigation is described on the enhancement of forced convection heat transfer using inclined thin plates as wing-type vortex generators in a rectangular channel. The channel constructed with these plates has diverging and converging parts along the main flow domain. Heat transfer coefficients and pressure drops were measured for air flow with various arrangements of the plates and Reynolds numbers. From experimental results, the usefulness of the design is determined and the most effective plate angle for the heat transfer enhancement is found. However, this techniques is also accompanied by large pressure drops. The large pressure drops in the converging-diverging channel (baffle passage) are related to flow separation in diverging parts of the channel. Hence, by narrowing the separation zone (baffle passage) it is expected that the pressure drop will decrease. The present authors propose a channel with slits (shown as g in Fig. 3), enlargements of winglet channel (shown as w in Fig. 3) of the converging and diverging parts in order to decrease pressure drop, and the performance of such a technique is evaluated. The geometries and positions of winglets are given in Figs. 2 and 3.

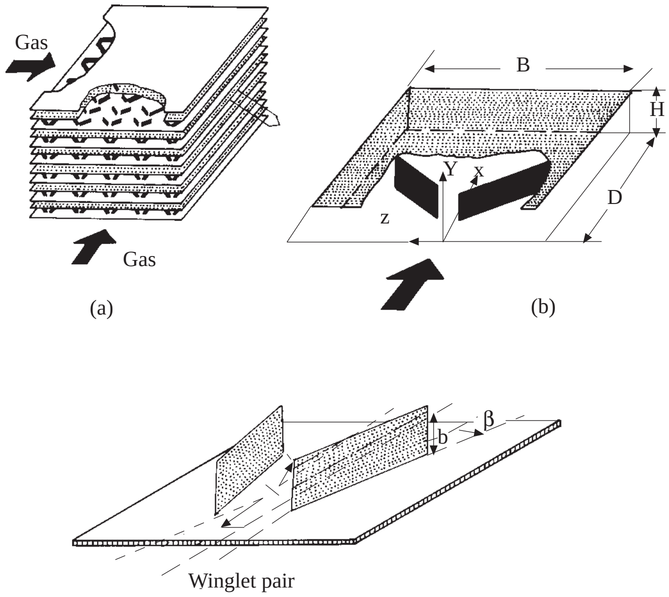

Figure 2. (a) Proposed flow domain that uses plate winglets, (b) coordinate system

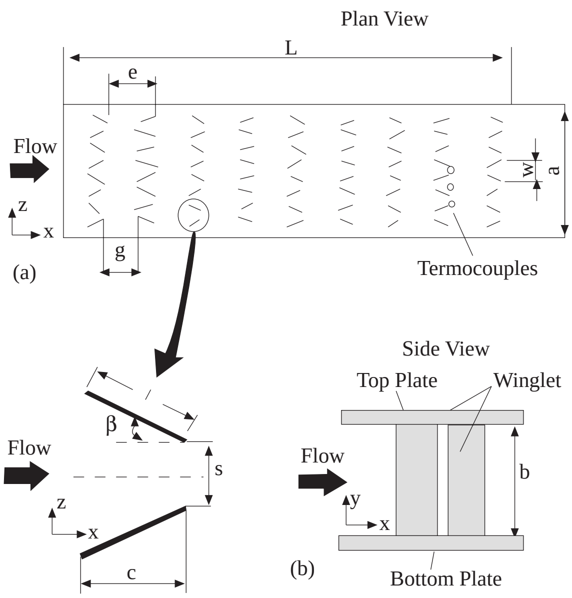

Figure 3. Geometry and placement of winglets between top and bottom walls of rectangular channel

Various geometric dimensions used in this study are given in Table 1, where the nomenclature used is noted on each figure with a symbol to identify each winglet. The work described here is believed to be the first fundamental-level study of periodically interrupted enlarged and contracted adjacent channels flow domain in rectangular duct.

Table 1. Characteristic parameters of the rectangular channel with wing-type vortex generator.

Channel type	Legend	b	a	l	g	s	w	β	e	L
TYPE REF	○	10	202	-	-	-	-	-	-	-
TYPE 1	□	10	202	60	10	9	23	7	67.5	655
TYPE 2	•	15	206	60	10	11	28	9	64.3	675
TYPE 3	Δ	18	215	60	10	10	33	11	68.8	660
TYPE 4	▼	20	226	60	10	12	55	15	71.0	640
TYPE 5	▲	20	210	60	10	13	48	20	80	650
TYPE 6	◊	10	210	60	10	10	10	0	70	660

Experimental apparatus and Procedures

Apparatus and Procedure

The main features of the test rig are shown schematically in Fig. 4. The apparatus consists of an air filter, a settling chamber, a hydrodynamic entrance section, a test section, a flexible pipe, an orifice plate and a fan. The experimental apparatus is operated in the suction mode. The test section is constructed with stainless steel plates, and outer surfaces of the channel is insulated electrically by means of fiberglass tape. The arrangement of winglets in the test section is shown in Fig. 3. Bottom and top plates of the rectangular duct are manufactured according to the dimensions given in Table 2 and shown in Fig. 3, and winglets are inserted through holes. Heating of the active length of the test section was achieved electrically using Nichrome resistance wire spirally wound over the outer periphery of the rectangular channels so that uniform heat flux is achieved. The outer surface of the test section was covered with a layer of glass-wool to inhibit external heat loss, and the entire section was covered with a protective shell of stainless steel. The rectangular duct has a cross sectional area of 10mmX208mm.

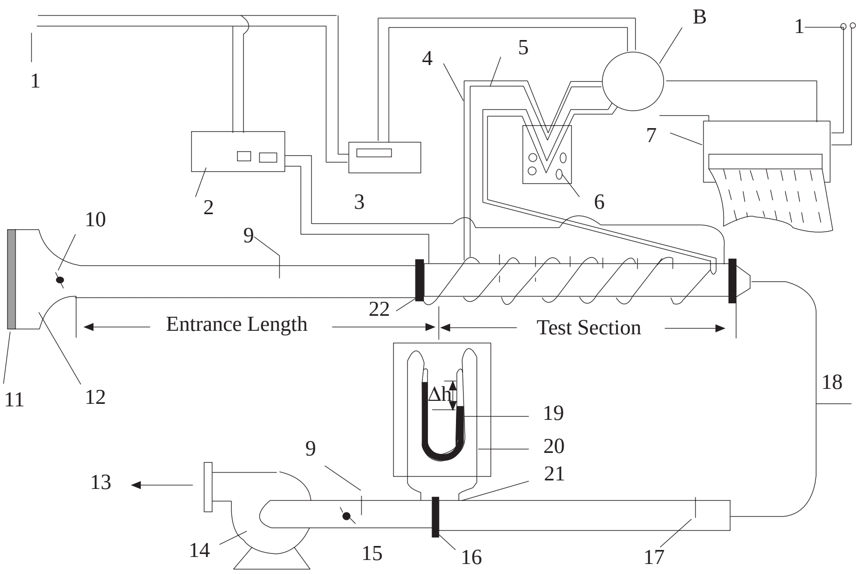

Figure 4. The main features of the test rig

The experiments were conducted in the test region. Air flows from the settling chamber to the inlet section of the duct (the entrance length is approximately 1500 mm), where the velocity is fully-developed. Then air travels into the test section of the thermal region. The test section is thermally insulated from entrance and outlet sections by special fiber flanges. At the end of the test section, air enters a convergent section which changes the cross-section from rectangular to circular. The circular duct section is made of a PVC pipe of 100 mm diameter and 2040 mm length which is connected to the convergent section through a flexible piping. A set of PVC companion flanges were then used to house the orifice plate. At the downstream of the orifice another section of PVC pipe of 100 mm diameter and 840 mm long was used feeding to the fan. This section contains a damper which can be adjusted to obtain the desired flow rate. To measure the pressure difference, pressure taps are mounted on the top plate of the rectangular duct similar to the test sections. The pressure taps are positioned on the center lines and mid points of converging and diverging channels. During the course of the experimental study, the power supply is kept constant at various Reynolds numbers. At a fixed value of heat input and for a given Reynolds number, the variations of the temperature along and transverse to the duct at different locations, air temperatures at the duct inlet and outlet, and before and after the orifice plate were recorded by a digital voltmeter and the eight-channel recorders. Experimental procedure for heat transfer can be outlined as follows:

(1) After the initial preparations mentioned above, the fan was turned on, the rate of flow through the test section was first set at the lowest desired values. The pressure difference across the orifice plate was recorded.

(2) Heat input was adjusted to a desired values by the variac in the power supply unit.

(3) After ensuring that the air is flowing through the system, the power supply was turned on. The various power levels desired was set at increasing order ending at the peak level.

(4) The temperature readings were periodically monitored to obtain temperature distributions. It was observed that stabilization of temperatures on the top wall of the duct was reached after at least one hour.

(5) After stabilization, all thermocouple voltages were recorded. The pressure drop across the orifice plate was also recorded so as to measure the flow rate. The atmospheric pressure was read from a mercury barometer.

(6) After completion of data recordings, the procedure was repeated, starting with step (2) again to carry out the experiments with the next Reynolds number value.

(7) Experiments were conducted for different Reynolds numbers at a fixed value of heat input. Same experimental procedure was applied to the smooth duct flow.

Instrumentation

Power supply for test section is measured by calibrated wattmeter. To measure the variation of temperature along x and z-direction of the duct, thermocouples were placed at equal intervals along the x and z directions from origin as shown in Fig. 4. The thermocouples, made from 30 gage, teflon-coated copper-constantan wires, were inserted in the holes drilled in the top wall. The height of holes is a half of wall thickness. The thermocouples were then sealed on the outside with a dab of silicon rubber. Thermocouples were also placed five-diameter-of-pipe away from the downstream face of orifice plate and at the inlet of the duct to measure the outlet and inlet temperatures of the air. After the reference junction (ice-point) the copper leads from all of the thermocouples were connected to a rotary thermocouple selector switch, then extended to an eight channel recorder unit. The ice-point thermocouple junctions were placed in an oil-filled glass tube immersed in a thermos bottle containing a mixture of ice and water. The mass flow rate was calculated from the pressure drop across the orifice plate obstruction meter which was constructed from brass and machined to standard specifications given by ASME standards (1984). The fan equipped with a 2.5 kW motor, 20 V AC, and has 100 mm inlet and outlet diametres. Once air passed through the fan, the air stream was routed up and out of the building by the use of flexible piping. Pressure differences along x and z directions were measured by using electronic micromanometer.

Flow Visualisation

The flow patterns as obtained from the flow visualisation test are presented in Fig. 5. Flow visualisation tests were used to explain the enhancement of heat transfer due to the various channel geometries. In the experiments, air and water were used as working fluids. In the Hele-Shaw apparatus, working fluid was water with a typical flow pattern for laminar main flow as seen in Fig. 5. Also, for flow visualisation tests with air, a smoke-generator was used for laminar main flow. Similar flow patterns were observed for the same channel geometry with water and air flows. The length of winglets and angles of inclination were kept constant during any particular test. In cases where the winglet angles is greater than 7°, a back-flow region forms just downstream end of the diverging section, indicating the occurrence of flow separation and presence of a recirculating zone (shown as A in Fig. 5). In addition, there is a region situated between diverging and converging channels (regions between A and B, in Fig. 5) where the velocity is too low to enable the resolution of the flow direction. Due to pressure rise at the end of the diverging channel (region A), and pressure drop at the neighboring converging channel(region B), the velocities were high enough to cause turbulence. This region is believed to be the mixing zone caused by the slit between divergent and convergent channel pairs.

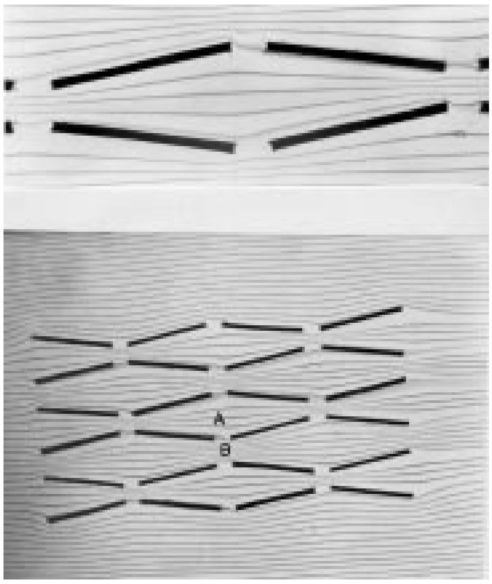

Figure 5. Flow patterns in periodically interrupted enlarged and contracted adjacent channels.

Data Reduction

Data collection during the experiments was carefully monitored so as to yield realistic and accurate results. For each experimental run, the data includes: (1) the pressure drop across the orifice plate observed in the U-tube manometer, (2) the pressure drop between inlet and outlet of test section by means of electronic-manometer, (3) the average temperature of air flow at a distance of five diameters away from the orifice plate, and (4) the temperatures at the top wall of the duct. (5) Air temperature at the inlet of the duct.

Reynolds Number

Mass flow rate through the PVC pipe was calculated by the use of the expression

$$\dot{m} = C\varepsilon_1 \frac{\pi}{4} d_p^2 (\frac{2\rho\Delta p}{1-\phi^4})^{0.5} \tag{1}$$

where Δp is the pressure drop across the orifice plate and C is the discharge coefficient
which is given by

$$C{=}0.5959{+}0.0312\phi^{2.1}{-}0.1840\phi^8{+}0.039\phi^4(1-\phi^4)^{-1} \\ -0.01584\phi^3{+}91.71\phi^{2.5}Re_p^{-0.75} \tag{2}$$

The coefficient ϵ_1 is the expansion factor (assumed unity, based on the present system configuration).
The Reynolds number Re_p in the PVC pipe was then calculated from:

$$Re_p = \frac{4\dot{m}}{\pi\mu D_p} \tag{3}$$

Iteration Procedure

Eqs. (1) and (3) can be combined to give

$$C = \frac{\mu D_p}{\epsilon_1 d_p^2}(\frac{2\rho\Delta p}{1-\phi^4})^{-0.5} Re_p \tag{4}$$

Thus finding the solutions to Eqs. (2) and (4) is equivalent to finding the intersection ($\dot{R}e_p, \dot{C}$) of the two curves. This was done by using an iteration procedure employing the golden section method (Ding 1986). After the iterated solution of $\dot{R}e_p$ is obtained, it is taken as the Reynolds number Re_p in the PVC pipe, and the mass flow rate $\dot{m}$ can be determined by Eq. (3) which is rearranged as

$$\dot{m} = \frac{\pi}{4}\mu D_p Re_p \tag{5}$$

The Reynolds number in the test section **Re** can then be determined by employing Re_p from

$$Re = \frac{\pi D_p \nu_p}{2(a+b)\nu_t} Re_p \tag{6}$$

Duct Friction Factor

Pressure drop measurements for the seven arrangements tested in this study were converted to friction factors. The following equation was used to calculate the friction factor:

$$f = \frac{\Delta p}{(\frac{L}{D_e})\frac{(\rho u^2)}{2}} \tag{7}$$

Duct Heat Transfer

The local heat transfer coefficient was calculated from the following equation:

$$h = \frac{q}{(T_w - T_m)} \tag{8}$$

where T_w is heated surface temperature, T_m is the bulk temperature, and q is the heat flux. T_m is evaluated by an energy balance calculation. The local Nusselt number Nu is defined as follows:

$$Nu = \frac{hD_e}{k} \tag{9}$$

where, k is the thermal conductivity at the bulk temperature. The local Nusselt number is to be evaluated at points along the test section in terms of the local heat flux, local difference in wall and bulk coolant temperatures, and the properties evaluated at the bulk temperature of the fluid. The local value of heat flux to the coolant was assumed to be the value of the external heat loss at any location which is directly proportional to the locally prevailing difference between the wall and ambient temperatures. The required constant of proportionality was taken from the previously determined heat loss calibrations. This procedure was acceptable since the heat loss calibrations were to be linear. The detailed explanation of the heat loss calibration technique was given by Ayhan (1982). The mean Nusselt number Nu_m is defined in terms of the mean flux and the mean difference between wall and fluid temperatures, with properties once more evaluated at the mean bulk temperature of the fluid.

Experimental Uncertainties

In the initial stages of investigation, a great deal of work was spent on calibration of measuring instruments in steady-state fluid flow. To adequately analyse the uncertainties associated with measured and/or calculated values, it is very important to evaluate the uncertainties inherent in a given experimental set-up in order to report results with the highest accuracy and reliability. Temperature measurements were made with standart copper-constantan thermocouples. Depending on bulb size, response time, velocity of air flow and thermocouple calibration polynomials, the total uncertainty associated with temperature measurements was estimated to be $\mp$ 0.1°C. This value is applicable when the temperature measurements is within the 0-100°C temperature range. Measurement of mass flow rate (m) and Reynolds number (Re_p, Re) were calculated from the pressure drop across the orifice plate in combination with the manometer calibration polynomial. The uncertainty associated with the mass flow rate arises from those in the orifice plate pressure drop, bulk mean fluid temperature, dimensions of the set-up, manometer calibration coefficients, and the thermal fluid properties. The total uncertainty associated with the mass flow rate and Reynolds number (Re) is resulted as 1 % in turbulent flow regime. Uncertainties in the Nusselt number were estimated according to the standard procedure (Ding, 1986).

Result and Discussions

In Fig. 6 and Fig. 7, the results for the rectangular channel without inserted winglets are presented to check the adequacy of experimental apparatus. Type Ref. is stood for the plain tube results which is satisfied Dittus-Boelter equations. The friction factor f and the average Nusselt number Nu_m are plotted as functions of Reynolds number in those figures. f and Nu_m were measured at the location where both flow and temperature fields are fully-developed. The results for the rectangular channel agree fairly well with the Petukov's formula, which is often used to estimate the pressure drop of the turbulent flow in the rectangular channel. The Petukov's formula is as follows:

$$f = (0.790 lnRe - 1.64)^{-2} \tag{10}$$

In Fig. 7, the Dittus-Boelter correlation, which is expressed by the following equation, is also plotted for comparison. It is shown as a continuous curve in Fig. 7.

$$Nu_m = 0.023 Re^{0.8} Pr^{0.4} \tag{11}$$

Here, Pr is the Prandtl number of air. The average Nusselt number is shown as a function of Reynolds number in Fig. 7. Good agreement between the results for the rectangular channel (TYPE REF) and these correlations is observed over a wide range of Reynolds number. It suggests that the experimental apparatus used in this study was adequate. The average Nusselt number increases with increasing the inclination angle. The Reynolds number dependence is almost the same as that of the rectangular channel. The heat transfer coefficient increase compared with the rectangular channel is about six times for TYPE 5, about 3 times for TYPE 4, respectively. Figure 6 shows the friction factor, where the Blasius correlation is also included for comparison. Due to the effect of the inclined winglets in the channel, the pressure drop also increases with increasing inclination angle. For all types of channel geometries, a dependence on Reynolds number can be seen and the value of f decreases with increasing Reynolds number. The friction factor of TYPE 5 is about 40 times that of rectangular channel.

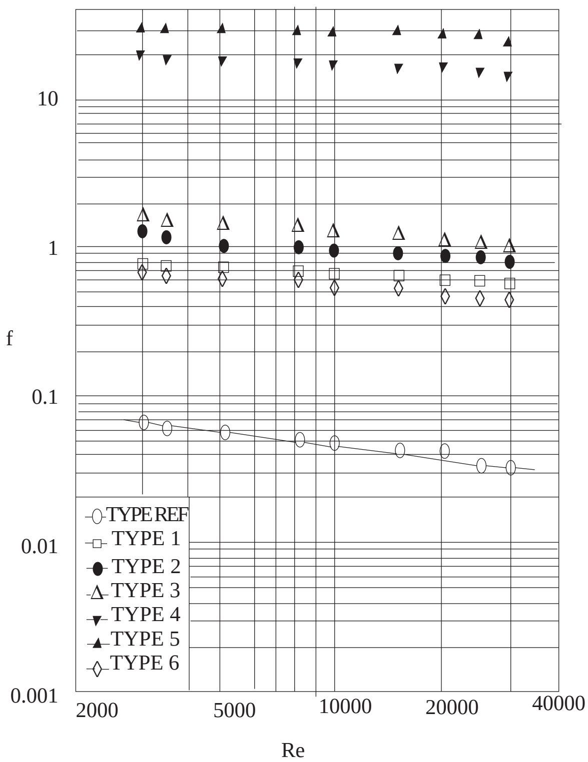

Figure 6. Effect of vortex generators on friction factors

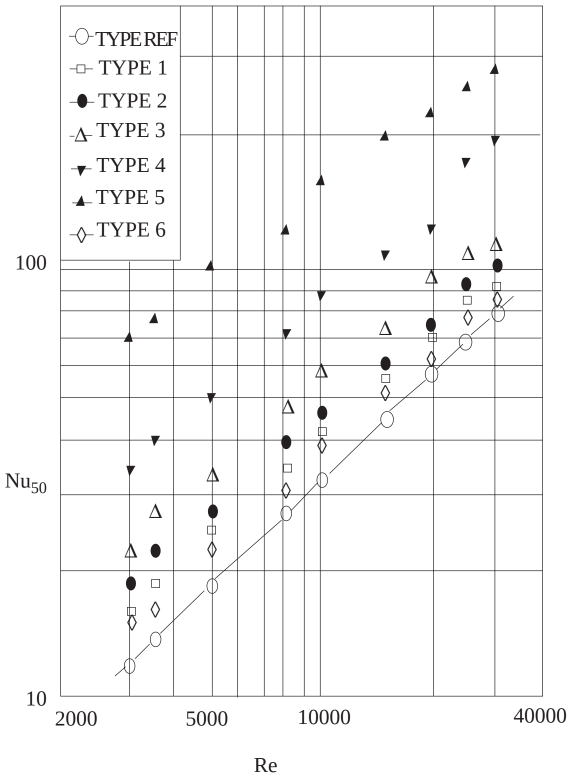

Figure 7. Effect of vortex generators on average Nusselt number Nu

Correlation for Rectangular Channel With Wing-Type Vortex Generator

In the preceding section, the effects of the winglet geometry on the heat transfer and pressure drop characteristics of rectangular channels were to some extent explained. Although the mechanism of the heat transfer on the heat exchanger surface was not fully understood, the authors attempted to establish the dimensionless correlations for the Nusselt number and the friction coefficient for practical purposes. The results are as follows:

$$Nu = 1.48Re^{0.63}(\frac{a}{b})^{0.70}(\frac{c}{L})^{0.65}(tan\beta)^{1.42} \quad (12)$$

$$f = C_0 Re^{-m} \quad (13)$$

for Pr=0.71 and 0< β <27°, in the range of 3000<Re<30000. The values of C_0 and m in the friction coefficient for each rectangular channel configuration are given in Table 2, where $0° < \beta < 20°$ and 3000<Re<30000. The experimental data were represented by the given correlations within the uncertainty of ∓8% for Nu and ∓10% for f.

Table 2. Coefficient for the friction factor correlations for wing-type rectangular channels

b	a	l	g	s	w	β	e	c	L	f:friction factor
10	202	60	10	9	23	7	68	59.6	655	2.84 $Re^{-0.166}$
15	206	60	10	11	28	9	64	59.3	675	7.06 $Re^{(-0.221)}$
18	215	60	10	10	33	11	69	58.9	660	11.08 $Re^{(-0.242)}$
20	226	60	10	12	55	15	71	59.7	640	74.27 $Re^{(-0.165)}$
20	210	60	10	13	48	20	80	56.4	650	77.82 $Re^{(-0.116)}$
10	210	60	10	10	10	0	70	60	660	4.00 $Re^{(-0.224)}$

Conclusions

From the results of the flow visualization, the mixing effect was expected in the intermediate region between wing cascades. It is due to the pressure and velocity differences across the passage between the converging pair of winglet and diverging pair of winglet. At each contraction part the boundary layer develops and at the end of the enlargement part, flow separation occurs. In these intermediate regions flow is turbulent. Thus, the heat transfer enhancement of the introduced rectangular channel geometries can be attributed to the secondary flow caused by the venturi type flow effect and the frequent boundary layer interruptions at each enlargement part. The effect of the introduced rectangular channel geometries were studied experimentally for different winglet arrangements. As the inclination angle of winglet increased the mixing effect in the intermediate region between wing cascades improves the heat transfer characteristics. The dimensions of the intermediate region between converging and diverging wing cascades is kept constant in all the tests. Thus, the mechanism of the heat transfer enhancement for these channel geometries coincided with the expectation from the results of the flow visualization. The dependence of Reynolds number on the friction factor is strong, the average Nusselt number increases by the Reynolds number. An increase of heat transer coefficient was observed with accompanying large pressure drops, increasing with the inclination angle. Finally, the dimensionless correlations (11) and (12) on the Nusselt number and the friction factor were derived. These correlations are expected to be useful for optimum design analyses of compact heat exchangers.

Acknowledgement

The authors wish to acknowledge support for this research by the Karadeniz Technical University Research Foundation under Research Grant No.93.112.0034

Nomenclature

a	:	width of the duct
b	:	height of the duct
c	:	length of winglet n x-direction
C	:	discharge coefficient
$\dot{C}$	:	iterative solution of discharge coefficient
C_0	:	friction coefficient for each rectangular channel configuration
D_p	:	diameter of PVC pipe, m
D_e	:	hydraulic diameter of the test section = 4.free flow area / wetted perimeter, m
d_p	:	diameter of the orifice plate, m
f	:	friction factor, dimensionless
k	:	thermal conductivity of air, W/mK
L	:	length of the test section
l	:	length of winglet
$\dot{m}$	:	mass flow rate, kg/s
Nu	:	Nusselt number, dimensionless
P	:	wetted perimeter, m
Δ P	:	pressure drop across the orifice plate, Pa
ΔP_a	:	pressure drop along the duct, Pa
ΔP_t	:	pressure drop transverse to the duct, Pa
Re_p	:	Reynolds number in the PVC pipe = $D_p.U_m/\nu$, dimensionless
$R\dot{e}_p$	:	iterative solution of Reynolds number = $D_p.U_m/\nu$, dimensionless
Re	:	Reynolds number in the test section = $D_e.U/\nu$, dimensionless
T	:	temperature, K
u	:	average velocity in the test section, m/s
u_m	:	average velocity in the PVC pipe, m/s
x, y, z	:	cartesian coordinates (x-flow direction, y-height direction of the duct), m

Greek Symbols

ϵ_1	:	expansion factor
ϕ	:	diameter ratio of the orifice plate = d_p/D_p
ρ	:	density, kg/m^3
μ	:	dynamic viscosity of air, Ns/m^2
β	:	inclination angle, degree
ν	:	kinemativ viscosity of air, m^2/s

References

Ayhan, T., “Sabit Isı Akışı Altında Borular İçindeki Akış için Yerel ve Ortalama Nusselt Sayısının Tayini için Deneysel Bir Yöntem”, Isı Bilimi ve Tekniği Dergisi, Cilt 5, Sayı 2, 1982.

Bergles, A.E., “Enhancement of Heat Transfer”, Int. J. Heat Transfer, 6, 89-168, 1978.

Bergles, A.E., “Augmentation of Heat Transfer”, Heat Exchanger Desing Handbook, 2, Hemisphere Washington D.C., 1983.

Bergles, A.E., Techniques to Augment Heat Transfer, Handbook of Heat Transfer Applications, 3-80, Mc. Graw-Hill, New york, 1985.

Deb P., Biswas, G. and Mitra, N.K., “Heat Transfer and Fluid Structure in Laminar and Turbulent Flows in a Rectangular Channel with Longitudial Vorticies”, Int. J. Heat and Mass Transfer, 38, No 13, 2427-2444, 1995.

Ding, Y., “Experimental Investigations of Transient Forced Convection in Ducts for a Timewise Varying Inlet Temperature”, Int. J. Heat and Mass Transfer, 29, 1495-1501, 1986.

Fuji, M., Sensimo, Y., Yamanaka, G., “Heat Transfer and Pressure Drop of Perforated Surface Heat Exchanger with Passage Enlargement and Contraction”, Int. J. Heat Mass Transfer, 31, 135-142, 1988.

Garg, V.K., Maji, P.K., “Laminar Flow and Heat Transfer in a Periodically Converging-Diverging Channel”, Int. J. for Numerical Methods in Fluids, 8, 579-597, 1988.

Maughan, J.R., Incropera, F.P., “Experiments on Mixed Convection Heat Transfer for Airflow in a Horisantal and Inclined Channel”, Int. J. Heat Mass Transfer 30, 1307-1318, 1987.

Mendes, P.S., Sparrow, E.M., “Periodically Converging-Diverging Tubes and Their Turblent Heat Transfer, Pressure Drop, Fluid Flow and Enhancement Characteristics”, Int. J. Heat Transfer, 106, 55-63, 1984.

Russels, C.M.B, Jones, T.V., Lee, G.H., “Heat Transfer Enchancement Using Vortex Generators”, Proceedings of the Seventh International Heat Transfer Conference, Munich, 3., 283-288, 1982.

Measurement of fluid flow in pipes using orifice, nozzle and venturi, ASME Standard, MFC - 3M - 1984.